J Mater Sci (2007) 42:4325–4333
DOI 10.1007/s10853-006-0470-4

Combustion and thermal properties of OctaTMA-POSS/PS composites

Lei Liu · Yuan Hu · Lei Song · Shonali Nazare · Shuqin He · Richard Hull

Received: 5 January 2006 / Accepted: 19 May 2006 / Published online: 28 February 2007

Abstract Inorganic–organic composites of octa (tetramethylammonium) polyhedral oligomeric silsesquioxanes (OctaTMA-POSS) and polystyrene (PS) were prepared by melt-mixing method. The composites were characterized by Fourier-transform infrared spectrometry (FT-IR), Transmission electronic microscopy (TEM), scanning electronic microscopy (SEM), and thermal gravimetric analysis (TGA). Their flammability was evaluated by cone calorimeter test. The experimental results indicate that OctaTMA-POSS, when present in low ratios (1%–5%, weight ratio) in the composites, can decrease the peak heat release rate (HRR) by 15%, while high ratios of OctaTMA-POSS (20% and 30%) can decrease the peak HRR and the average HRR approximately linearly. Concentration and release rate of carbon monoxide (CO) in the composites combustion are also decreased evidently. Thermal gravimetric analysis under nitrogen and air atmosphere both show that the char yield increases obviously. These advances are attributed to the special properties of OctaTMA-POSS and its dispersion in PS.

L. Liu · Y. Hu (✉) · L. Song · S. He
State Key Laboratory of Fire Science, University of Science & Technology of China, Hefei, Anhui 230027, China
e-mail: yuanhu@ustc.edu.cn

S. Nazare · R. Hull
Centre for Materials Research and Innovation, The University of Bolton, Deane Road Bolton, Greater Manchester BL3 5AB, UK

Introduction

Polymer is widely used in our everyday life, but its application is frequently limited due to its flammability. Substantive research work has been carried out on flame-retarded polymer composites [1–5], yet it also remains a great challenge how to improve their flame-retarded property and thermal stability. Usually different additives are added into polymer in order to improve their flame retardation [6–12]. As one of the most extensively-used resins, polystyrene (PS) has attracted much attention with respect to its thermal stability and flame-retarded property [13–27]. Thus by improving its flame-retarded property while keeping its mechanic and dynamic properties, we can significantly enlarge its application extension. Previous research work has revealed that through the heat release rates (HRR), mass loss rates (MLR) and smoke production rates (SPR), flame retardation of PS composites can be dramatically decreased comparing to pure PS [28]. For PS, synergic systems made of Sb_2O_3 and halogen exhibit excellent flame-retarded performance [29, 30], but they are still unsatisfying if we take their impact on environment into account. Therefore, the silicon-containing flame-retarded polymer composites appear promising, owing to their enhanced properties over the base polymer and environment-friendliness [31–34].

Silsesquioxanes are a large branch of organic–inorganic silicon containing compounds. Generally speaking, there are three main kinds of structures in silsesquioxanes: random structures, ladder-like structures and cage-like structures (including partial cage-like structures). They can be represented as $(RSiO_{3/2})n$, where R can be hydrogen or any alkyl, alkylene, aryl,

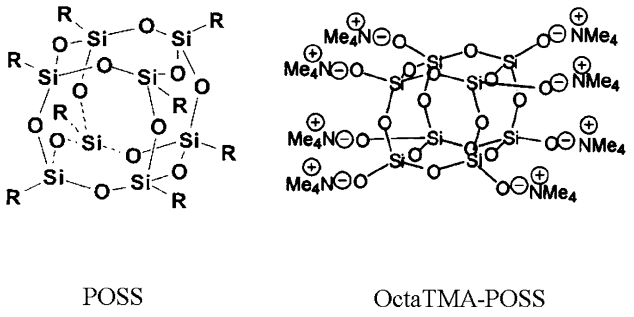

POSS OctaTMA-POSS

Scheme 1 Polyhedral Oligomeric Silsesquioxanes (POSS) and Octa(tetramethylammonium) Polyhedral Oligomeric Silsesquioxanes (OctaTMA-POSS)

arylene groups, or organo-functional derivatives of them [35, 36]. The great variety of the side group R can result in the diversity of silsesquioxanes [37]. For this reason, a lot of novel chemical materials with high thermal stability and good mechanic properties have been synthesized based on silsesquioxanes since the last century [38–41]. One of the most popular branches of silsesquioxanes is polyhedral oligomeric silsesquioxanes (POSS, its structure is given in Scheme 1), including T8 cage, T10 cage, T12 cage and other partial cage structures. Laine and his coworkers [42–47] have synthesized many kind of organic–inorganic composites based on POSS, while Tabuani presents an extensive study to evaluate the influence of the POSS substituent groups on the morphological and thermal characteristics of melt-blended POSS/PP composites [48]. Till now only a little work has been reported so far with regards to polymer nanocomposites prepared with non-reactive POSS.

OctaTMA-POSS which contains a substituted T8 POSS cage is bestowed potential flame retardation on polymeric materials due to its special structure and composition. Further more, non-halogen and non-phosphorus containing structure suggests that it is environment friendly. In this work, we used OctaTMA-POSS as an additive to obtain PS composites with improved flame-retarded properties and thermal properties.

Experimental section

Materials

Tetramethylammonium hydroxide with crystal water was obtained from Xinde Chemical Plant (Zhejiang, China) and was purified by re-crystallization prior to use. Tetraethoxysilane was commercially available and was of analytical grade. Polystyrene was friendly supplied by Hefei Keyan Chemical Materials Company.

Techniques

Infrared spectra were obtained by using a MAGNA-IR 750 spectrometer. Thermal gravimetric analysis (TGA) was performed on a Netzsch STA-409c Thermal Analyzer under a 50×10^3 mm^3/min nitrogen or air flow with the heating rate of 10 °C/min. SEM and TEM images were obtained from X-650 scanning electronic microscope system and H-800 transmission electronic microscope system respectively. The combustion properties of OctaTMA-POSS/PS composites were evaluated by using a cone calorimetry test. All samples ($100 \times 100 \times 3$ mm^3) were exposed to a Stanton Redcroft cone calorimeter under a heat flux of 35 kW/m^2. The experiment was carried out according to ISO-5660 standard procedures [49]. The cone data reported here is the average of three replicated experiments. Limiting oxygen index (LOI) determination was performed on a HC-2 LOI testing device (Jiangsu, China) according to ASTM D2863. Test specimens ($100 \times 6.5 \times 3$ mm^3) were cut from pressed plates. MALDI-TOF data was acquired on a GCT gas chromatography time-of-flight mass spectrometer at the pressure of 0.280 Pa under a certain heating program.

Synthesis of OctaTMA-POSS and OctaTMA-POSS/PS composites

OctaTMA-POSS was synthesized according to the reported procedures [44]: First, 108.8 g $(CH_3)_4NOH{\cdot}5H_2O$ was dissolved in 438.6 g deionized water, into which 125.0 g tetraethoxysilane was slowly dropped under mechanical stirring. After been kept at room temperature (25 °C) for 24 h, the temperature of the reaction system was raised to 60 °C under mechanical stirring. Six hours later, the reaction solution was condensed by partial pressure distillation and then it was placed in a refrigerator at 2 °C. OctaTMA-POSS with crystal water was crystallized from the condensed solution little by little. Its ideal structure was shown in Scheme 1. Then OctaTMA-POSS was dried in a vacuum oven at 80 °C in order to eliminate its crystal water. It was milled and selected by a sieve. At last, OctaTMA-POSS and PS were added into an internal mixer (XK-160, Jiangsu, China). The roll speed was controlled at 50 rpm, the temperature was maintained at about 130 °C, and the total mixed time was 20 min. The obtained composites were desiccated in a vacuum oven at 100 °C for 24 h.

Results and discussion

Characterization of OctaTMA-POSS

OctaTMA-POSS is crystallized from the reaction solution system. The desiccated OctaTMA-POSS can be easily dissolved in water and re-crystallization again, which is an evidence for the maintenance of its cage-like structure. FTIR spectrum of dried OctaTMA-POSS (white powder) is showed in Fig. 1-d. The five main absorbing peaks at 2945 cm^{-1}, 1648 cm^{-1}, 1491 cm^{-1}, 1401 cm^{-1}, 1037 cm^{-1} can be attributed to the stretching vibration of saturated C–H bond, MeNO group, MeN group and Si–O bond respectively, while one peak at 936 cm^{-1} stands for the torsional vibration of MeN group.

TGA curves for OctaTMA-POSS with crystal water and without crystal water under nitrogen are showed in Fig. 2. OctaTMA-POSS containing crystal water starts to lose weight at the beginning of the temperature rising, while degradation of OctaTMA-POSS without crystal water doesn't occur until 200 °C, as a result of the decomposition of $–N(CH_3)_4$ group of POSS. After 300 °C, TG curve reaches a flat. At 500 °C, the ratio of residual weight is 48.3%. It should be noted that the relative molecular weight of the inside POSS core made up of silicon and oxygen atoms is 544, which is 47.9% of that of OctaTMA-POSS (Its relative molecular weight is 1136). The coincidence indicates that all the organic part of OctaTMA-POSS has decomposed completely when the temperature is higher than 300 °C.

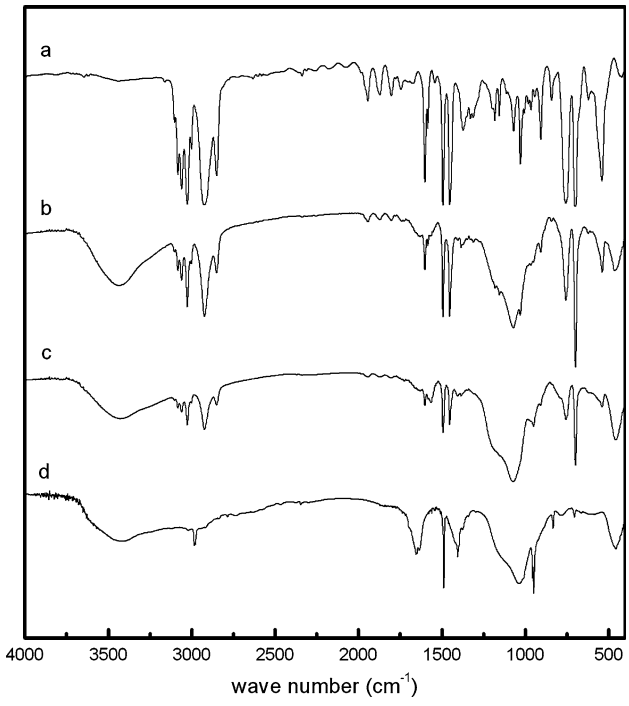

Fig. 1 FTIR spectrum of dried OctaTMA-POSS and OctaTMA-POSS/PS composites: **(a)** PS; **(b)** 20% OctaTMA-POSS/80%PS; **(c)** 30% OctaTMA-POSS/70%PS; **(d)** OctaTMA-POSS

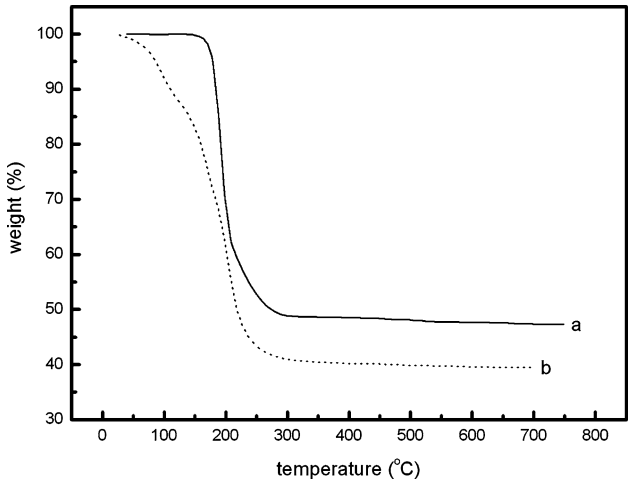

Fig. 2 TGA data for **(a)** OctaTMA-POSS without crystal water and **(b)** OctaTMA-POSS with crystal water

Characterization of OctaTMA-POSS/PS composites

OctaTMA-POSS/PS composites were characterized by FTIR (Fig. 1) and TEM (Fig. 3a–d). In FTIR spectra, the absorbing peaks related to PS (the peaks around 3000 cm^{-1}, the peaks at 1942 cm^{-1}, 1870 cm^{-1}, 1802 cm^{-1}, 766 cm^{-1}, 697 cm^{-1}, etc.) and the absorbing peaks belonging to OctaTMA-POSS (the peaks at 2945 cm^{-1}, 1648 cm^{-1}, 1491 cm^{-1}, 1401 cm^{-1}, 1037 cm^{-1}, etc.) can all be found in the spectra for composites, and the relative intensity of the absorbing peaks approximately matches their ratios.

From TEM images of the composites, OctaTMA-POSS nanofibre can be found in PS base when the weight ratio of OctaTMA-POSS in the composites rises to a certain amount. OctaTMA-POSS is one kind compound with cage-like structure, with one silicon atom in each of the eight corner of the cubic cage, and each silicon atom is connected with one $–ON(CH_3)_4$ group. So there must be a lot of hydrogen bond and strong electrostatic attraction between positive and negative charges in the composites. The core of the cage is made up of silicon and oxygen atoms, together with eight $–ON(CH_3)_4$ groups at the corner of the cage, which is a very rigid structure. Strong molecular force between groups and the rigid core of OctaTMA-POSS structure will help it assemble linearly. All these

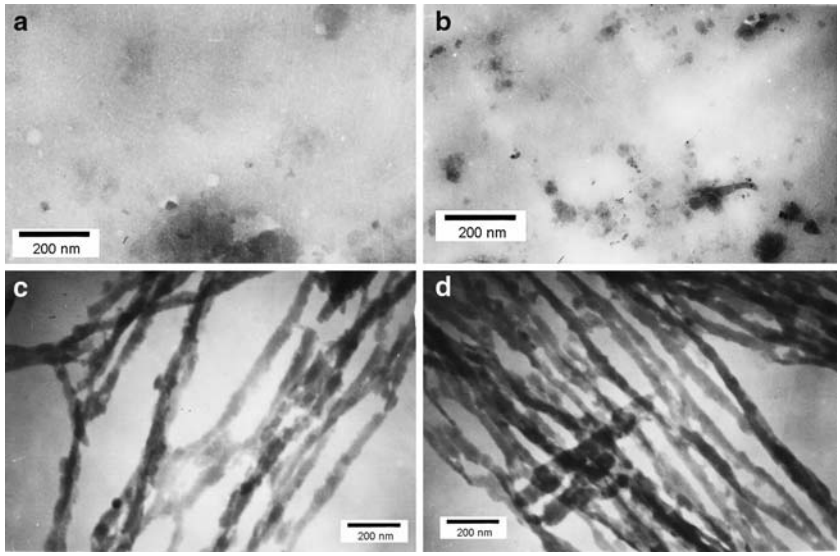

Fig. 3 TEM images of POSS/PS composites: **(a)** 1% OctaTMA-POSS/99% PS; **(b)** 5% OctaTMA-POSS/95% PS; **(c)** 20% OctaTMA-POSS/80%PS; **(d)** 30% OctaTMA-POSS/70%PS

factors are favorable for the formation of the nanofibre structures in the polymer substrate. Further more, rotor of internal mixer can provide strong shearing force in the preparations, which can make the nanofibre structures disperse in the polymer homogeneously.

Enhanced combustion properties of OctaTMA-POSS/PS composites

The cone calorimeter is one of the most effective bench-scale methods to study the inflammabilities of materials. The common adopted parameters for fire hazard evaluation of materials in cone calorimeter test are heat release rate (HRR), peak heat release rate (pHRR), total heat release (THR), fire index grow rate (FIGRA), time to ignition, etc., among which HRR, especially pHRR is regarded as the most important parameter [50]. In our experiment, small ratios of OctaTMA-POSS can decrease the pHRR of the composites (Fig. 4) obviously, but there are little differences between samples with OctaTMA-POSS content from 1% to 5%. When the ratios of OctaTMA-POSS are raised to 20% and 30%, the pHRR of the composites drops approximately linearly (Fig. 5). There is 31.7% descent for Composite-2 (20%OctaTMA-POSS/80%PS) and 54.6% descent for Composite-3 (30%OctaTMA-POSS/70%PS) respectively when compared to pure PS. Especially for Composite-3, a fat occurs in the HRR curve, which is a distinct contrast with the sharp peak of pure PS in HRR. When the peak heat release rate at different ratios are observed, it can be found that the peak HRR and average HRR drop nearly linearly versus the OctaTMA-POSS ratios

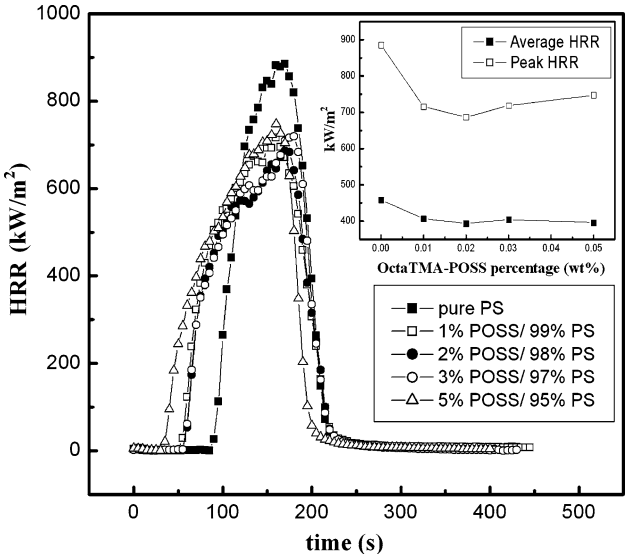

Fig. 4 The heat release rate (HRR) results of OctaTMA-POSS/PS composites with low POSS weight ratios (from 1% to 5%). The radiant power is 35 kW/m^2

(Fig. 5, here we employ composite-1 (5%OctaTMA-POSS/95%PS) as comparison in order to find out the variation tendency of the peak HRR and the average HRR.). It is speculated that little amount of OctaTMA-POSS is not enough to form continuous structure in PS, but when the weight ratio increases to a certain amount, consecutive organic–inorganic nanofibre is formed, which can separate the base polymer into small units at nanometer scale. The OctaTMA-POSS clapboard can prevent heat and mass from quick transferring in the composites, which improves the combustion and thermal proprieties of the composites

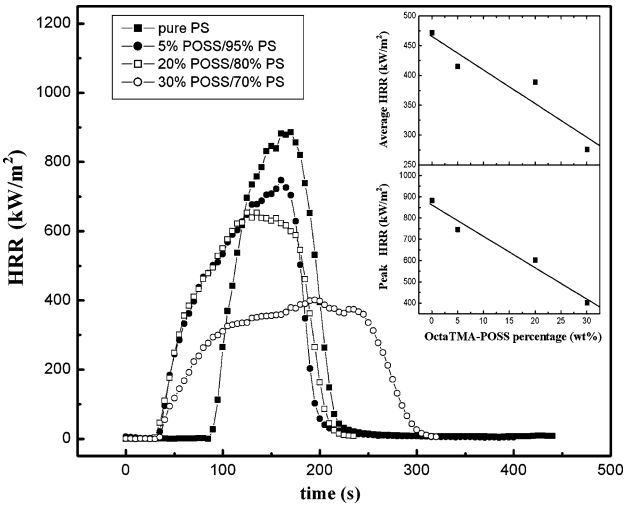

Fig. 5 The heat release rate (HRR) results of OctaTMA-POSS/PS composites with high POSS weight ratios (from 5% to 30%). The radiant power is 35 kW/m^2

effectively. In the mass loss rate curve obtained in the combustion course (Fig. 6), we can also perorate that OctaTMA-POSS slows down the mass loss rate of the composites combustion markedly.

The obvious decrease of the peak HRR, average HRR and mass loss rate of composites is attributed to OctaTMA-POSS in the composites. During the combustion process, the organic part of OctaTMA-POSS is oxidized, accompanied by the release of the generated volatiles such as carbon dioxide, vapor and nitrogen containing derivatives. As we known, there are two stages in the combustion of polymer: the long carbon chains breach stage and the flammable gases combustion stage. Oxidation of the organic part of OctaTMA-POSS consumes oxygen and leads to the formation of

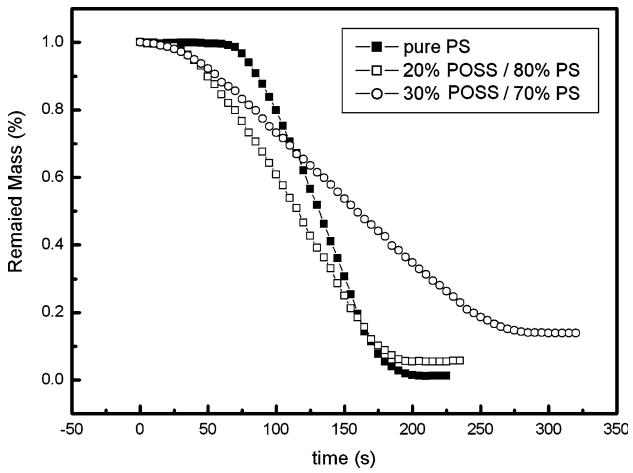

Fig. 6 The mass loss rate of OctaTMA-POSS/PS composites in the combustion

the compact inorganic layers made of silicon oxide in the composites, which can limit the amount of oxidant provided to inner PS and thereby delay the oxidation and combustion of base polymer. On the other hand, the flammable gases generated by unit mass of OctaTMA-POSS in decomposition is less than that generated by unit mass of PS, which can decrease the concentration of the flammable gases during composites degradation. Further more, the organic part of OctaTMA-POSS will degrade into trimethylamine, which will finally degrade into ammonia (inert gas) under heating and the local conditions limited oxygen (this will be further explained in the following discussion). Gases generated from OctaTMA-POSS degradation result in the intumescences of composites, which is confirmed by SEM images of residue char (Fig. 7a, b). All of these factors will help the composites to get a lower heat release rate and a lower mass loss rate. At the same time, limited oxygen index (LOI, %) of the composites is increased from 17 to 23. The main improvements are list in Table 1, and the data reported here is the average of three replicated experiments. These improvements of combustion properties for the composites are attributed to the OctaTMA-POSS added into PS.

The peak CO release rate (PCORR) and peak CO concentration (PCOC) in the combustion are also obviously decreased. 1%, 2%, 3%, 5% OctaTMA-POSS in the composites make PCORR decrease by 51.2%, 53.1%, 50.7%, 52.7% respectively. When the ratios rise to 20% and 30%, PCORR can be decreased by 66.2% and 70.8% respectively (Fig. 8). In the same way, 1%, 2%, 3%, 5% OctaTMA-POSS in the composites make PCOC in the combustion decrease by 35.7%, 39.1%, 36.1%, 38.9% respectively. When the ratios rise to 20% and 30%, PCOC can be decreased by 55.3% and 66.1% respectively (Fig. 9). These obvious enhancements in the combustion properties improve the fire safety performance of PS composites.

Thermal degradation and thermal oxidation of OctaTMA-POSS/PS composites

TGA curves in Figs. 10 and 11 describe the weight loss process of composites with high OctaTMA-POSS ratios under nitrogen and air atmosphere respectively. Relevant parameters in TGA are list in the Table 2. From Fig. 10 we can see, although the thermal degradation of the composites begins from about 250 °C, the main decomposition temperature remains at about 420 °C. OctaTMA-POSS enhances the char residue of composites significantly. For pure PS, almost nothing is left when the temperature is more than 600 °C, while

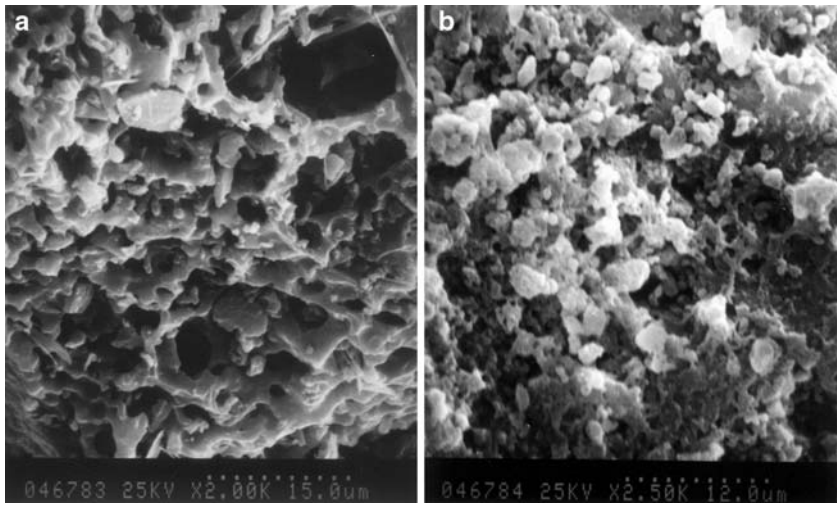

Fig. 7 SEM images of OctaTMA-POSS/PS composites combustion char residue: **(a)** for 20% OctaTMA-POSS/80%PS **(b)** for 30% OctaTMA-POSS/ 70%PS

Table 1 Thermal and combustion properties of POSS/PS composites

Sample	Peak of HRR (kW/m^2)	Average HRR (kW/m^2)	Peak of CO release rate (μg/s) ($\times 10^{-4}$)	Peak of CO concentration ($\times 10^{-6}$)	Limited Oxygen Index (LOI, %)
Pure PS	882.9 ± 40.1	472.1 ± 20.1	252.6 ± 12.6	1763.7 ± 78.2	17.0 ± 0.5
Composite-1	747.3 ± 34.3	396.3 ± 14.8	154.4 ± 6.7	837.2 ± 31.8	18.0 ± 0.5
Composite-2	602.6 ± 14.6	388.8 ± 19.0	109.9 ± 4.5	599.0 ± 24.9	22.0 ± 0.5
Composite-3	401.4 ± 19.2	276.0 ± 10.3	85.7 ± 2.3	516.5 ± 19.8	23.0 ± 0.5

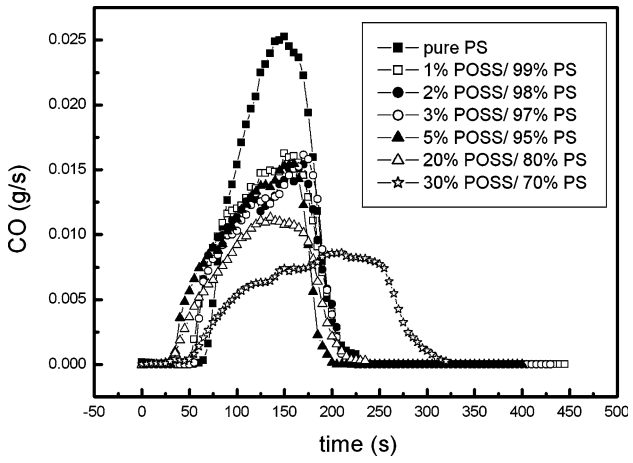

Fig. 8 CO concentration in the combustion of OctaTMA-POSS/ PS composites

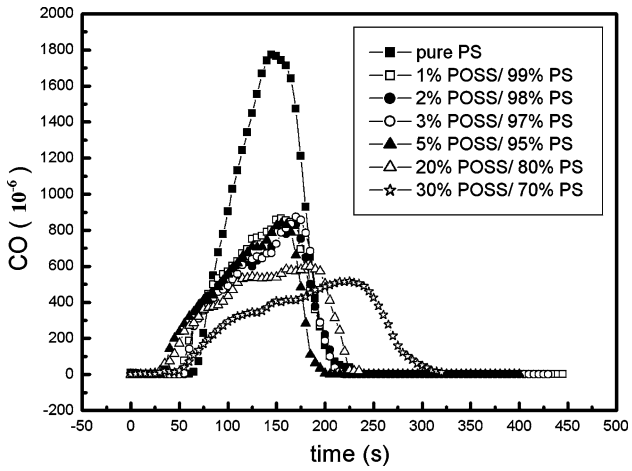

Fig. 9 CO release rate curve in the combustion of OctaTMA-POSS/PS composites

for Composite-2 and Composite-3, there are 22.8% and 28.1% char left respectively. Deduction the effects of OctaTMA-POSS decomposition, which should eliminate about 51.8% from OctaTMA-POSS component itself (see it in Fig. 2), the char of composites has been raised by 7.2% and 13.8% for Composite-2 and Composite-3 respectively. Further more, OctaTMA-POSS also can reduce the decomposition rate of the composites. As we can see in the differential thermal gravimetric analysis (DTG) curve (Fig. 12), the peak decomposition rate reduces from 29.1%/min (for pure PS) to 23.0%/min (for Composite-2) and 19.7%/min (for Composite-3), and the temperature corresponding to maximal mass lost rate rises about 9 °C when compared to pure PS. The reduction of decomposition rate suggests the improvement in thermal stability of

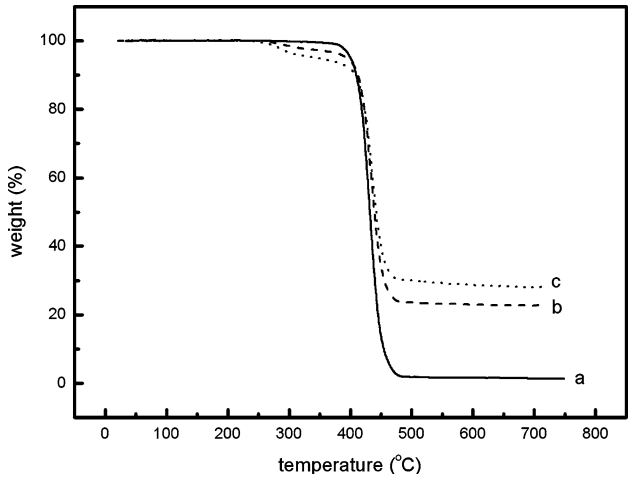

Fig. 10 The thermal gravimetric analysis results of OctaTMA-POSS/PS composites in nitrogen: **(a)** pure PS; **(b)** 20%OctaTMA-POSS/80%PS **(c)** 30%OctaTMA-POSS/70%PS

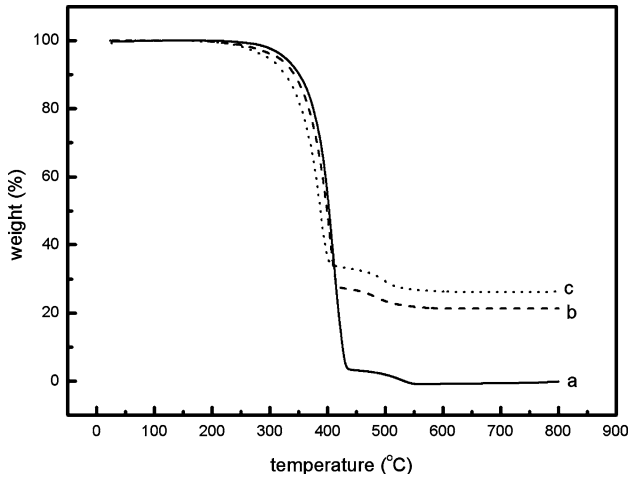

Fig. 11 The thermal gravimetric analysis results of OctaTMA-POSS/PS composites in air: **(a)** pure PS; **(b)** 20%OctaTMA-POSS/80%PS **(c)** 30%OctaTMA-POSS/70%PS

the composites, which can be attributed to OctaTMA-POSS. The organic–inorganic component made up of silicon and oxygen in the cage-like framework can decrease the thermal conductivity of PS, prevent heat from fast spreading in the composites. In this way, the gasification and decomposition rate are cut down.

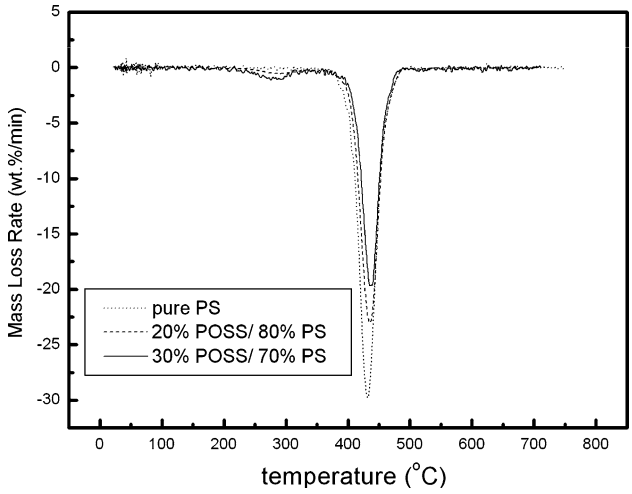

Fig. 12 The differential thermal gravimetric analysis (DTG) of OctaTMA-POSS/PS composites: **(a)** pure PS; **(b)** 20%OctaTMA-POSS/80%PS **(c)** 30%OctaTMA-POSS/70%PS

Because there is no new bond formed in the composites, PS and OctaTMA-POSS are connected by intermolecule force, the main degradation temperature of composites does not change obviously.

The thermal oxidation of the composites is investigated by TGA under air atmosphere. The results indicate that OctaTMA-POSS help to raise the char residue of the composites evidently (Fig. 11). There are 21.3% and 26.2% increase of char residue for Composite-2 and Composite-3 respectively. The decomposition temperature of the composites is reduced due to the decomposition of OctaTMA-POSS. The relevant data obtained from TGA are list in Table 2 and the data reported here is the average of three replicated experiments. The real-time IR spectrum of composite-3 (Fig. 13) matches the TGA results well. The composite begins to decompose from 300 °C to 350 °C, and the char residue can be determined as silicon oxide at 450 °C.

Possible mechanism of flame property improvement

The accession of OctaTMA-POSS into PS results in the improved flame-retarded properties of the

Table 2 Main parameters obtained from TGA curves of composites

Sample	In nitrogen atmosphere			In air atmosphere		
	5% Weight loss temperature (°C)	50% Weight loss temperature (°C)	700 °C Char yield (%)	5% Weight loss temperature (°C)	50% Weight loss temperature (°C)	700 °C Char yield (%)
Pure PS	400.1 ± 1.3	431.5 ± 2.4	1.4 ± 0.1	325.9 ± 1.2	402.9 ± 1.9	0
Composite-2	391.9 ± 1.2	438.8 ± 2.1	22.8 ± 0.6	314.5 ± 1.3	399.2 ± 1.5	21.3 ± 0.5
Composite-3	344.1 ± 1.5	442.2 ± 1.8	28.1 ± 0.8	296.3 ± 0.9	388.2 ± 2.1	26.2 ± 0.4

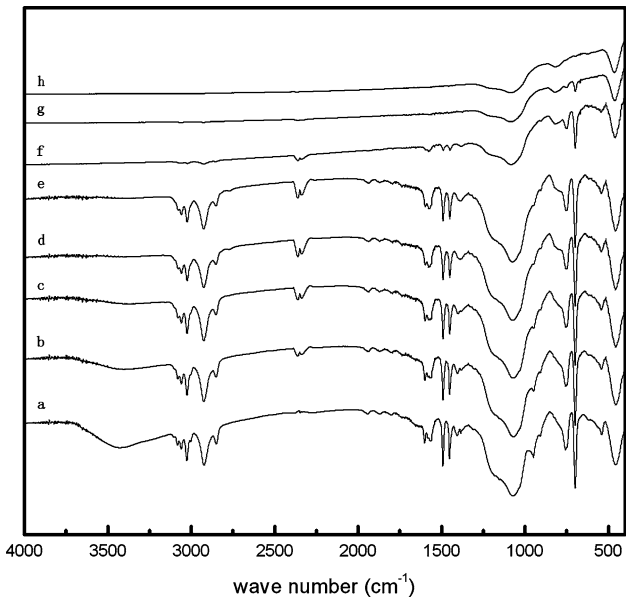

Fig. 13 The real-time IR spectrum of 30%OctaTMA-POSS/70%PS: **(a)** rt; **(b)** 150 °C; **(c)** 200 °C; **(d)** 250 °C; **(e)** 300 °C;**(f)** 350 °C; **(g)** 400 °C; **(h)** 450 °C

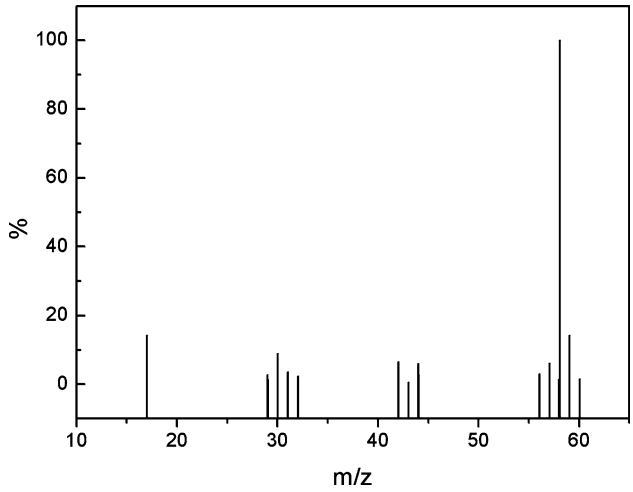

Fig. 14 Mass spectrum of OctaTMA-POSS obtained under 250 °C, 0.280 Pa and programming heating

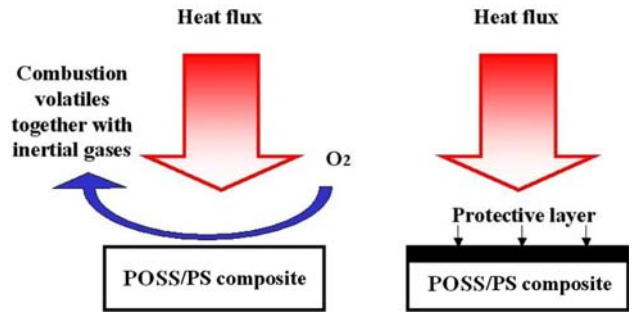

Scheme 2 the sketch combustion course of OctaTMA-POSS/PS composites

composite, such as the decrease of peak HRR, average HRR, peak CO release rate, peak CO concentration and the obvious increase of char residue. Based on the experimental results, the mechanism of these improvements can be deduced as following: (1) OctaTMA-POSS begins to decompose at 200 °C, which absorbs a great deal of heat. This slows the temperature rising of the polymer and delays the decomposition and combustion of the composites. (2) The inert gas generated from the degradation of OctaTMA-POSS in combustion will dilute the mixture of flammable gases and oxygen. They will take away part of heat from the combustion system. Figure 14 shows the mass spectrum of OctaTMA-POSS obtained at 250 °C (MALDI-TOF (m/z): 17, 29, 30, 31, 32, 42, 43, 44, 56, 57, 58, 59, 60; [$N(CH_3)_3$ = 59 amu, $NH(CH_3)_2$ = 44 amu, NH_2CH_3 = 30 amu, NH_3 = 17 amu]). It suggests that –$ON(CH_3)_4$ groups of OctaTMA-POSS degrade into trimethylamine (TMA, $N(CH_3)_3$) when the composites are heated but not ignited. The generated $N(CH_3)_3$ is under the surrounding and protection of unburned PS, which provides a temporary local condition lack of oxygen. TMA will further degrade into organic volatiles, such as dimethylamine, methylamine and NH_3 finally, which is a kind of inert gas. These inflammable and uninflammable gases generated from OctaTMA-POSS degradation result in the obvious intumescent effect, which can be testified by porous structure in SEM images of char (Fig. 7). (3) The large amount of silicon and oxygen components in OctaTMA-POSS constitutes inorganic layers when organic part of OctaTMA-POSS has degraded completely. It will partially cover the surface of PS. The uninflammable and adiabatic inorganic layers disperse in the inner of composites continuously or discontinuously, which prevent the flammable gases from entering the combustion system and prevent PS from further oxidization. This can be illustrated in Scheme 2.

Summary

Organic–inorganic OctaTMA-POSS/PS composites with improved combustion properties and more char yield were synthesized by melt-blending method. Comparing to pure PS, peak HRR of the OctaTMA-POSS/PS composites has been cut down by 54.5% and average HRR of the composites has been cut down by 41.5%. The char of the composites in the TGA test under nitrogen and air atmosphere both have a notable

increase. These improvements are result from the particular netlike structure formed in the composites. It can also be expected that with other proper fire resistant cooperation, composites with better combustion properties can be obtained.

Acknowledgements We wish to thank the National Natural Science Foundation of China (No.50403014), Specialized Research Fund for the Doctoral Program of Higher Education (20040358056) and Bolton Fellowship supported by The University of Bolton, UK for financial support.

References

1. Giancaspro J, Balaguru P, Lyon R (2004) SAMPE J 40:42
2. Zhang H, Westmoreland PR, Farris RJ, Coughlin EB, Plichta A, Brzozowski ZK (2002) Polymer 43:5463
3. Brzozowski ZK, Kijenska D, Zatorski W (2002) Des Monomers Polym 5:183
4. Bourbigot S, Flambard X, Ferreira M, Poutch F (2002) J Fire Sci 20:3
5. Chen-Yang YW, Lee HF, Yuan CY (2000) J Polym Sci – Pol Chem 38:972
6. Srinivasan S, Kagumba L, Riley DJ, Mcgrath JE (1997) Macromol Symp 122:95
7. Kumar D, Khullar M, Gupta AD (1993) Polymer 34:3025
8. Gilman JW, Bourbigot S, Shields JR, Nyden M, Kashiwagi T, Davis RD, Vanderhart DL, Demory W, Wilkie CA, Morgan AB, Harris J, Lyon RE (2003) J Mater Sci 38:4451
9. Bourbigot S, Vanderhart DL, Gilman JW, Awad WH, Davis RD, Morgan AB, Wilkie CA (2003) J Polym Sci Pol Phys 41:3188
10. Bourbigot S, Gilman JW, Wilkie CA (2004) Polym Degrad Stabil 84:483
11. Lee A, Lichtenhan JD (1999) J Appl Polym Sci 73:1993
12. Lee A, Lichtenhan JD (1998) Macromolecules 31:4970
13. Zhang J, Zhang HP (2005) J Fire Sci 23:193
14. Chen DZ, Yang HY, He PS, Zhang WA (2005) Compos Sci Technol 65:1593
15. Braun U, Schartel B (2005) J Fire Sci 23:5
16. Balabanovich AI (2004) J Fire Sci 22:163
17. Balabanovich AI, Levchik GF, Yang JH (2002) J Fire Sci 20:519
18. Braun U, Schartel B (2004) Macromol Chem Physic 205:2185
19. Simonson M, Tullin C, Stripple H (2002) Chemosphere 46:737
20. Levchik SV, Bright DA, Moy P, Dashevsky S (2001) J Vinyl Addit Techn 6:123
21. Murashko EA, Levchik GF, Levchik SV, Bright DA, Dashevsky S (1998) J Fire Sci 16:233
22. Boscoletto AB, Checchin M, Milan L, Pannocchia P, Tavan M, Camino G, Luda MP (1998) J Appl Polym Sci 67:2231
23. Benrashid R, Nelson GL, Ferm DJ (1994) J Fire Sci 12:529
24. Boscoletto AB, Checchin M, Tavan M, Camino G, Costa L, Luda MP (1994) J Appl Polym Sci 53:121
25. Boscoletto AB, Checchin M, Milan L, Camino G, Costa L, Luda MP (1993) Makromol Chem-M Symp 74:35
26. Roma P, Luda MP, Camino G (1993) Makromol Chem-M Symp 74:299
27. Checchin M, Boscoletto AB, Camino G, Luda MP, Costa L (1993) Makromol Chem-M Symp 74:311
28. Liu XF, Zhang J, Zhang HP (2004) Acta Polym Sin 5:650
29. Bhaskar T, Matsui T, Uddin MA, Kaneko J, Muto A, Sakata Y (2003) Appl Catal B-Environ 43:229
30. Jakab E, Uddin MA, Bhaskar T, Sakata Y (2003) J Anal Appl Pyrol 68–69:83
31. Devaux E, Rochery M, Bourbigot S (2002) Fire Mater 26:149
32. Bartholmai M, Schartel B (2004) Polym Advan Technol 15:355
33. Connell JE, Metcalfe E, Thomas MJK (2000) Polym Int 49:1092
34. Liu TM, Baker WE, Langille KB, Nguyen DT, Bernt JO (1998) J Vinyl Addit Techn 4:246
35. Laine RM (2005) J Mater Chem 15:3725
36. Baney RH, Itoh M, Sakakibara A, Suzuki T (1995) Chem Rev 95:1409
37. Li GZ, Wang LC, Ni HL, Pittman CU (2001) J Inorg Organomet P 11:123
38. Fina A, Tabuani D, Carniato F, Frache A, Boccaleri E, Camino G (2006) Thermochim Acta 440:36
39. Liu L, Hu Y, Li XK, Chen ZY, Fan WC (2005) Thermochim Acta 438:164
40. Mya KY, Huang J, Xiao Y, He CB, Siow YP, Dai J (2003) Abstr Pap Am Chem S 226:U528–U529 448-PMSE Part 2
41. Constable GS, Lesser AJ, Coughlin EB (2004) Macromolecules 37:1276
42. Choi J, Yee AF, Laine RM (2003) Macromolecules 36:5666
43. Tamaki R, Tanaka Y, Asuncion MZ, Choi JW, Laine RM (2001) J Am Chem Soc 123:12416
44. Choi J, Harcup J, Yee AF, Zhu Q, Laine RM (2001) J Am Chem Soc 123:11420
45. Tamaki R, Choi J, Laine RM (2003) Chem Mater 15:793
46. Kim SG, Choi J, Tamaki R, Laine RM (2005) Polymer 46:4514
47. Laine RM, Choi J, Lee I (2001) Adv Mater 13:800
48. Fina A, Tabuani D, Frache A, Camino G (2005) Polymer 46:7855
49. ISO 5660-1993 (1993) Fire test-reaction to fire part I: Rate of heat release from building products (Cone Calorimeter Method). International Standards Organization (ISO), Geneva
50. Babrauskas V, Peacock RD (1992) Fire Safety J 18:255